Biophysical Chemistry 15 (1982) 223–234
Elsevier Biomedical Press

HEAVY METAL-NUCLEOTIDE INTERACTIONS

15. REACTIONS OF CALF THYMUS DNA WITH THE ELECTROPHILES METHYLMERCURY(II) NITRATE, *cis*-DICHLORODIAMMINEPLATINUM(II), AND *trans*-DICHLORODIAMMINEPLATINUM(II) STUDIED USING RAMAN DIFFERENCE SPECTROSCOPY

EVIDENCE FOR THE FORMATION OF C-DNA UPON METALATION

T. O'CONNOR [a], M. BINA [b], D.R. McMILLIN, M.R. MOLLER HALEY and R.S. TOBIAS [†]

Department of Chemistry, Purdue University, West Lafayette, IN 47907, U.S.A.

Received 12th November 1981

Key words: DNA structure; Antitumor drug; Mutagen; Raman spectroscopy; Methylmercury(II); Dichlorodiammineplatinum(II)

This study details the reactions of the electrophiles $CH_3Hg(NO_3)$, *cis*-$[PtCl_2(NH_3)_2]$ (*cis*-DDP) and *trans*-$[PtCl_2(NH_3)_2]$ (*trans*-DDP) with calf thymus DNA using Raman and Raman difference spectroscopy. The order of $CH_3Hg(II)$ binding to calf thymus DNA is G≫T>C>A. The electrophilic attack of *cis*- and *trans*-DDP on calf thymus DNA produces different orders of binding: *cis*-DDP-G>C≈A≫T, *trans*-DDP-G≈C≈A≫T. The reaction of $CH_3Hg(II)$ with DNA results in a decrease in the percentage of B-form DNA, whereas the reactions of *cis*- and *trans*-DDP with DNA decrease the percentage of B-DNA and cause the formation of C-DNA structure.

1. Introduction

The binding of Hg(II) and Pt(II) complexes to DNA has been under extensive investigation in recent years [1–5]. Hg(II) is a mutagen which binds to DNA bases [2], but more recently, as a consequence of the monofunctional binding and rapid substitution kinetics of the $CH_3Hg(II)$ cation [6–11], studying $CH_3Hg(II)$ binding to nucleic acid species has proved useful for fingerprinting binding sites on bases. $CH_3Hg(II)$ has been postulated to react first at N(3) of thymidine and then N(1) of guanine, consistent with thermodynamic arguments [12,13]. The binding properties of the Pt(II) species, *cis*-$[PtCl_2(NH_3)_2]$ (*cis*-DDP) with nucleic acids have been investigated because *cis*-DDP is an antineoplastic drug which selectively inhibits DNA synthesis by binding to DNA bases [14–20]. In contrast, the geometric isomer, *trans*-

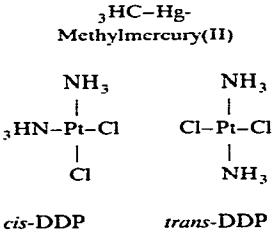

Scheme 1.

[a] Present address: Department of Biochemistry, University of Wisconsin-Madison, 420 Henry Mall, Madison, WI 53706, U.S.A.

[b] To whom correspondence should be addressed.

[†] Deceased February 1980.

0301-4622/82/0000–0000/$02.75

$[PtCl_2(NH_3)_2]$ (*trans*-DDP), has demonstrated no antitumor activity [19]. Differences in the reactivities of *cis*- and *trans*-DDP, therefore have been used to infer mechanisms for *cis*-DDP activity [21]. The *cis*- and *trans*-DDP reactions with nucleic acids are also important because these complexes have been used to make heavy metal derivatives for X-ray diffraction work on oligo- and polynucleotides [22–25]. Both platinum complexes react at the N(7) of guanine followed by reaction with either or adenine [1–5,26].

Previously, we have extensively studied the reactions of heavy metals and the proton with monomeric nucleosides and nucleotides using Raman difference spectroscopy and have characterized fingerprints for reactions at the various ring nitrogens [6,7,10,27]. In general, the binding of different metal complexes to identical sites on a base produces similar Raman difference spectra [11]. We [10,26] and others [28] have used Raman spectroscopy to probe metal-DNA structure and have shown that Raman spectroscopy can provide structural information concerning binding sites, base stacking and conformation [27]. This work completes the series of fingerprint spectra for the monomers, uses the fingerprints to interpret the binding of $CH_3Hg(II)$, *cis*-DDP and *trans*-DDP to calf thymus DNA, and uses Raman spectroscopy to show conformation changes of DNA.

2. Experimental

2.1. Metal complexes

2.1.1. CH_3HgNO_3

CH_3HgI was purchased from Alfa and checked for purity by examining the ^1H-NMR spectrum in benzene. $CH_3Hg(II)NO_3$ was prepared by adding a solution of $AgNO_3$ to a stoichiometric amount of $CH_3Hg(II)I$ and stirring overnight at room temperature. AgI was removed by filtration through sintered glass. The concentration of $CH_3Hg(II)$ was determined by atomic absorption spectroscopy.

2.1.2. *cis- and trans*-$[PtCl_2(NH_3)_2]$

Syntheses of *cis*-DDP and *trans*-DDP were by the methods of Dhara [29] and Kauffman and Cowan [30], respectively. The purity of the complexes was checked by elemental analysis (theoretical: N, 9.34; H, 2.02; Cl, 23.63). The analyses of *cis*-DDP and *trans*-DDP showed the following percentages: *cis*-DDP: N, 9.33; H, 2.02; Cl, 23.46 and *trans*-DDP: N, 9.15; H, 2.15; Cl, 23.80. The Raman spectra of the solid complexes were also compared with reference spectra [31].

2.2. Nucleic acids

The 5'-AMP and 5-GMP ribonucleotides were purchased from Sigma Chemical Co. and used without further purification. The calf thymus DNA was purchased from the Sigma Chemical Co., St. Louis, MO and PL Biochemicals, Inc., Milwaukee, WI. When necessary the DNA was purified by washing the fibers with portions of 70% ethanol/water to remove salts. The washing was repeated and the ethanol removed by lyophilization.

The concentrations of the DNA solutions used in this study were determined by ultraviolet spectroscopy at 260 nm assigning $a_p = 6600$ cm^2/mol P [32]. The pH of the DNA solutions was 7.0 as measured by a Radiometer PHM 64 pH meter.

2.3. Metal complex/DNA solutions

The $CH_3Hg(II)$ solutions were prepared by pipetting an aliquot of 15 mM DNA into a vial and adding the appropriate amount of 0.1 M CH_3HgNO_3; the pH was adjusted to 7.0 by addition of NaOH. The $CH_3Hg(II)$/DNA mixtures were then transferred to an Amicon model 8 MC ultrafiltration system and concentrated to approx. 60 mM in phosphate using Amicon membrane filters (UM10, UM20, or XM50).

The *cis*- or *trans*-DDP was reacted in the solid form with 12.1 mM calf thymus DNA. The mixtures were prepared by weighing the complex in 3-ml centrifuge tubes followed by addition of the calf thymus DNA. The reaction mixtures were allowed to equilibrate for a period of 1 week at 25°C and then stored at 4°C till spectra were secured. The spectra of DNA interacting with *cis*- and *trans*-DDP were recorded without concentrating the reaction mixtures.

2.4. Raman spectra

Raman spectra and Raman difference spectra were obtained using two different Raman instruments. Raman spectra of $CH_3Hg(II)$ were recorded using a system based on a Jobin-Yvon Ramanor HG-2 monochromator, and Raman spectra of *cis*- and *trans*-DDP species were recorded using a system based on a Spex 1400 monochromator. The Jobin-Yvon system used a Coherent Cr-8 Ar^+ laser for sample irradiation while the Spex system had a Cr-52G Ar^+ and a Lexel Model 95 Kr^+ laser. Both systems were controlled by the same Data General Nova II minicomputer. The spectra data were processed either off-line using Program Raman [33] or with Nova Software [34]. Further instrumental details are given in ref. 34–36. The $CH_3Hg(II)$ spectra were recorded using 514.5 nm excitation, but the 647.1 nm krypton laser line was used to obtain spectra of *cis*- and *trans*-DDP complexes because excitation at 514.5 nm resulted in photoreduction of Pt(II) to elemental platinum. The $CH_3Hg(II)$/DNA solutions used 25–85 mM NO_3^- as an internal frequency standard, whereas the *cis*- and *trans*-DDP/DNA solutions used 4 mM sodium cacodylate as an internal frequency standard. Other experimental details are included in the figure legends.

3. Results and discussion

The Raman difference spectrum produced by electrophilic attack at adenine, guanine, cytosine, or thymine is characteristic for a given base, specific for a ring nitrogen binding site, and nearly independent of electrophile.

Previous studies in our group [6–11,27a] have examined the binding sites of electrophiles on ring nitrogen positions at N(1) of adenine, N(1) of guanine, N(7) of guanine, N(3) of thymine, and N(3) of cytosine by using $CH_3Hg(II)$, *cis*-DDP, *trans*-DDP, and protonation. Here we have completed the series by determining the Raman difference spectrum for the binding of *cis*-DDP to the N(7) of 5'-AMP. Thus, we have been able to construct an entire series of Raman difference spectrum 'fingerprints' which reflect the binding of almost any electrophile to a particular base site (fig. 2). Those fingerprints have allowed us to conduct a detailed investigation on the order of binding of $CH_3Hg(II)$, *cis*-DDP, and *trans*-DDP to a native, double-stranded DNA. Furthermore, we have analyzed the effect of metalation on the conformation of the double helix.

3.1. Binding of cis-DDP to N(7) of 5'-AMP

To determine the fingerprint Raman difference spectrum for N(7) electrophilic attack on 5'-AMP (see scheme 2) we took advantage of the inert kinetics of *cis*-DDP [37] and the protonation of the N(1) of AMP at pH 2 [38] to direct the binding of *cis*-DDP to the N(7) of 5'-AMP. We used the following scheme. We reacted the *cis*-DDP with 5'-AMP at pH 2.0 in a 1:1 ratio until the reaction ceased and then raised the pH of the solution to 7.0 and recorded the Raman spectrum. The Raman difference spectrum for N(7) metalation of 5'-AMP was formed by subtracting the Raman spectrum of unreacted 5'-AMP at pH 7.0 from the Raman spectrum of the mixture at pH 7.0, since at neutral pH protons are released from the N(1) position, but the *cis*-DDP remains bound. The Raman difference spectrum for the N(7) reaction

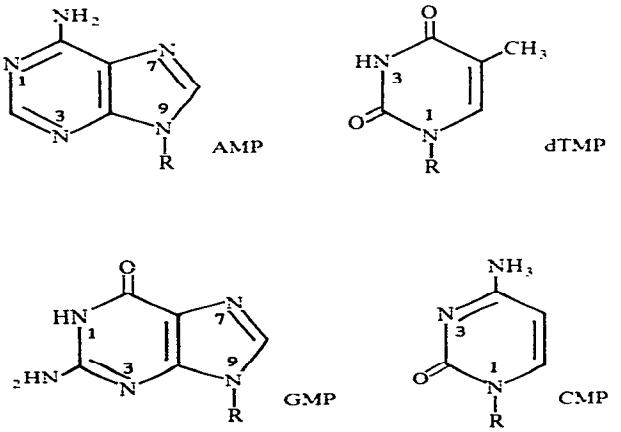

Scheme 2.

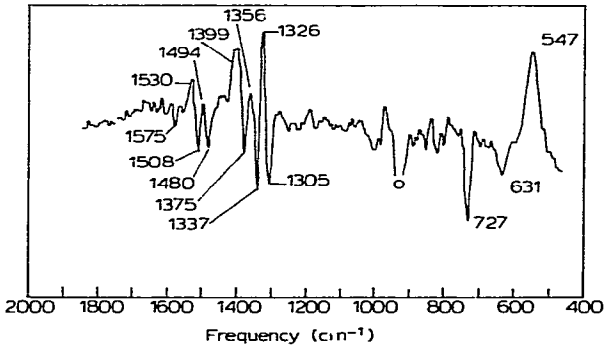

Fig. 1. Raman difference spectrum of 5'-AMP (25 mM) platination at the N(7) position. The *cis*-DDP binding at N(7) was induced by reaction at pH 2. The pH was then raised to pH 7 to remove the proton from the N(1) position. The *cis*-DPP:5'-AMP ratio was 1.0. The o reflects the mismatch of the perchlorate concentration between the platinated AMP and the 5'-AMP reference. The spectral slit width was 6.0 cm^{-1} at 647.1 nm. Data were obtained by scanning at 10 s/step in 1 cm^{-1} steps. Spectra were subjected to two-cycle, 17-point quartic, Savitsky-Golay smoothing [50].

on 5'-AMP shown in fig. 1 exhibits bands at 1480 and 1530 cm^{-1}. This completes the assignment of the Raman difference spectra for ring nitrogen binding of electrophiles.

We have summarized all the available data in fig. 2 in the form of line Raman difference spectra and used those data to interpret the binding of $CH_3Hg(II)$, *cis*-DDP and *trans*-DDP to native calf thymus DNA.

3.2. *Binding of $CH_3Hg(II)$ to calf thymus DNA*

To follow the spectral changes which result from the binding of $CH_3Hg(II)$ to DNA, we con-

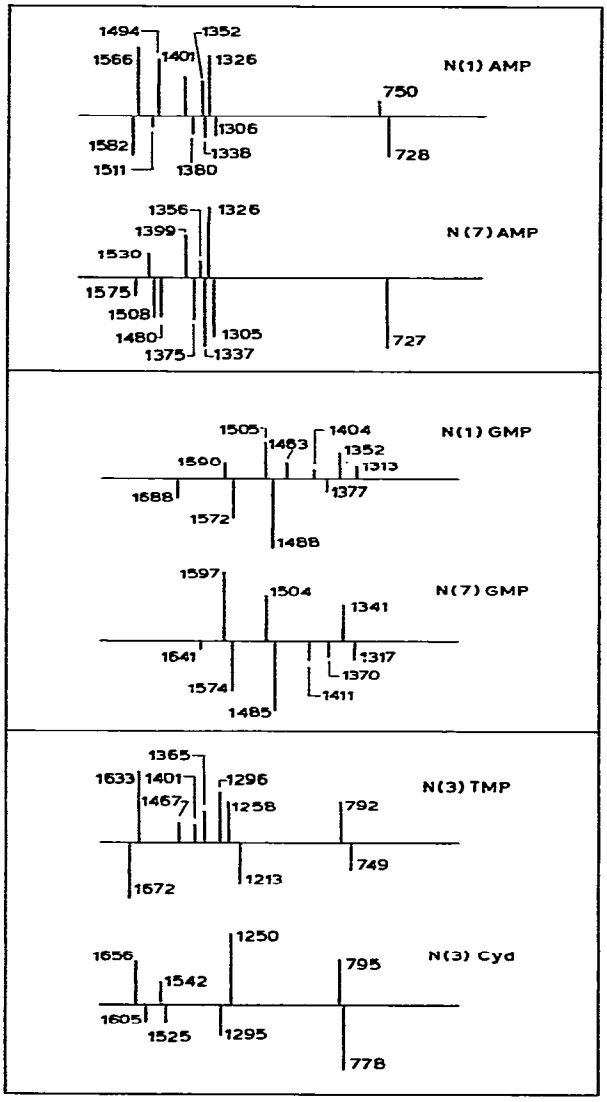

Fig. 2. Raman difference line spectra for electrophilic attack on ring nitrogens of nucleic acids. The Raman difference spectrum frequencies are indicated on the figure. This figure is a compilation of the Raman difference spectra for several different works (refs. 11, 26 and 39, and this paper), therefore, the wave number values may be considered accurate only to ±3–4 cm^{-1}, since the binding of different electrophiles results in small differences in frequency [11,26]. These bands do not include bands associated with metal-ring nitrogen or internal electrophile vibrations. Metal-ring nitrogen and internal electrophile vibrations generally are not helpful in the determination of binding sites because those bands are only slightly perturbed when electrophiles bind [6–11,26]. However, Raman bands of the electrophiles are often intense and several examples of vibrations associated directly with electrophiles appear in the spectra in this investigation. The symmetric Hg-C stretching vibration, and the methyl group bending vibration have bands at approx. 561 and 1204 cm^{-1}, respectively [6–11]. The bands which are observed in the spectra of *cis*- and *trans*-DDP complexes between 520 and 550 cm^{-1} are also examples of Pt-N vibrational bands associated with the Pt(II) electrophiles [11,26].

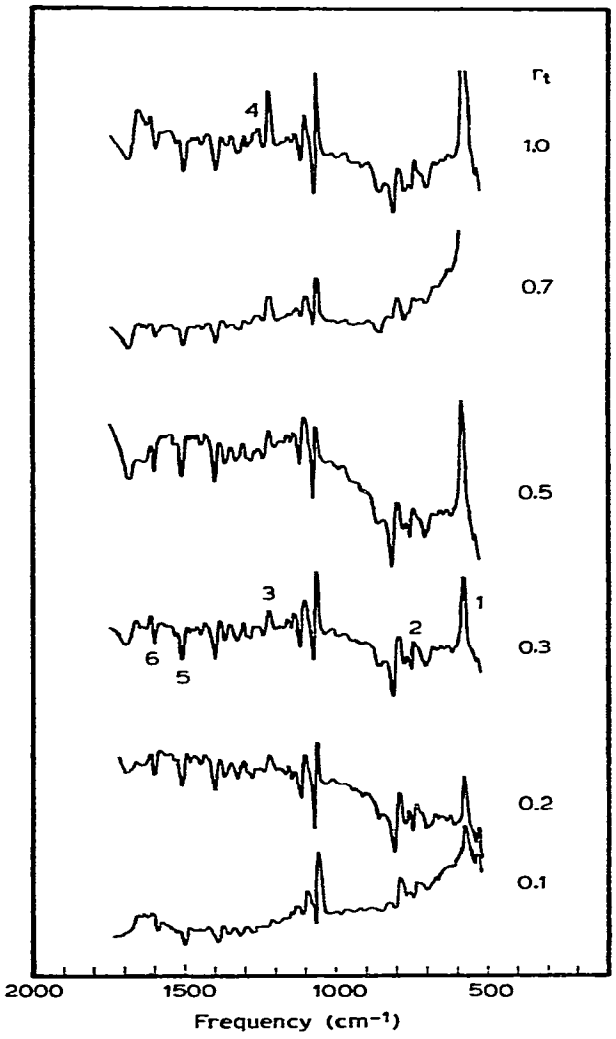

Fig. 3. Raman difference spectra of calf thymus DNA reacted with $CH_3Hg(II)$. The spectral slit width was 3.9 cm^{-1} at 514.5 nm. Spectra were formed by subtraction of the $r_t = 0$ spectrum from the spectra at higher r_t values. Data were obtained by scanning at 10 s/step in 1 cm^{-1} steps. Spectra were subjected to two-cycle, 21-point quartic, Savitsky-Golay smoothing [50]. The r_t values are indicated on the figure. The frequencies are listed in table 1. The numbered bands are: (1) 561, (2) 728, (3) 1206, (4) 1247, (5) 1492 and (6) 1586 cm^{-1}.

Table 1

Raman frequencies for Raman difference spectra in fig. 3 of calf thymus DNA reacting with $CH_3Hg(II)$ in H_2O

$r_t = 1.0$ (cm^{-1})	
Peaks	Valleys
561	799
799	1383
1206	1492
1247	1586
1289	1680
1332	
1366	
1603	
1645	

structed Raman difference spectra by subtracting the $r_t = 0$ ($r_t = [metal]_{total}/[phosphate]_{total}$) spectrum from the spectra at higher r_t values (fig. 3). At r_t values below 0.2, the two bands at 1492 and 1582 cm^{-1} have intensity values which suggest binding to guanine residues. The low intensity of the band at approx. 1600 cm^{-1} is consistent with binding at the N(1) of guanine as indicated by fig. 2 [39].

We also were interested in the carbonyl region, 1600–1700 cm^{-1}, of the Raman difference spectrum which provides information on thymine binding. In order to obtain high-quality difference spectra in the above region, the $CH_3Hg(II)$ was reacted with DNA in ^2H_2O to shift interfering water bands. The Raman difference spectra in fig. 4, constructed from the Raman spectra in

Table 2

Raman frequencies for Raman difference spectra in fig. 4 of calf thymus DNA reacting with $CH_3Hg(II)$ in ^2H_2O

$r_t = 1.0$	
Peaks	Valleys
561	1483
789	1577
1209	1618
1337	1675
1509	
1601	
1646	

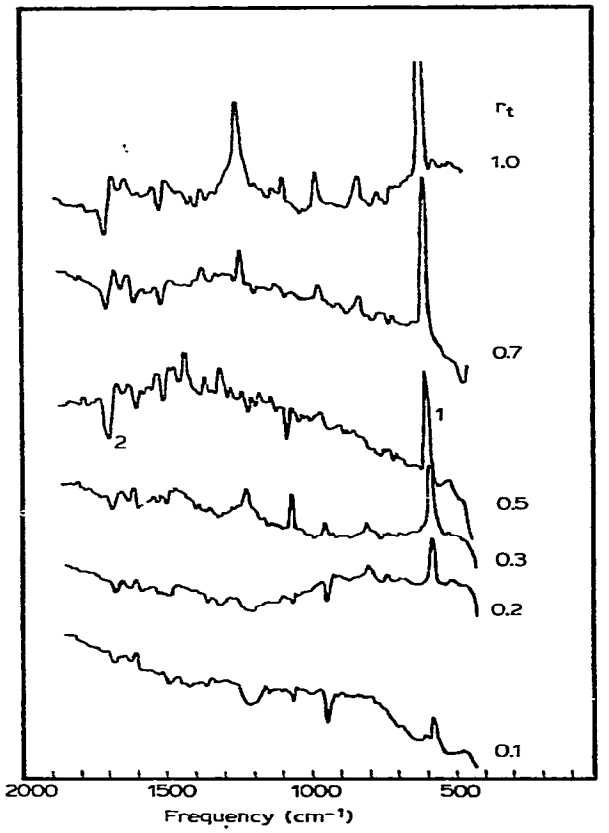

Fig 4. Raman difference spectra of calf thymus DNA reacted with $CH_3Hg(II)$ in ^2H_2O. The spectral slit width was 3.9 cm^{-1} at 514.5 nm. Spectra were formed by the subtraction of the $r_t = 0$ spectrum from the spectra of higher r_t values. Data were obtained by scanning at 10 s/step in 1 cm^{-1} steps. Spectra were subjected to two-cycle, 21-point quartic, Savitsky-Golay smoothing [50]. The r_t values are indicated in the figure. The frequencies are listed in table 2. The numbered bands are: (1) 561 and (2) 1675 cm^{-1}.

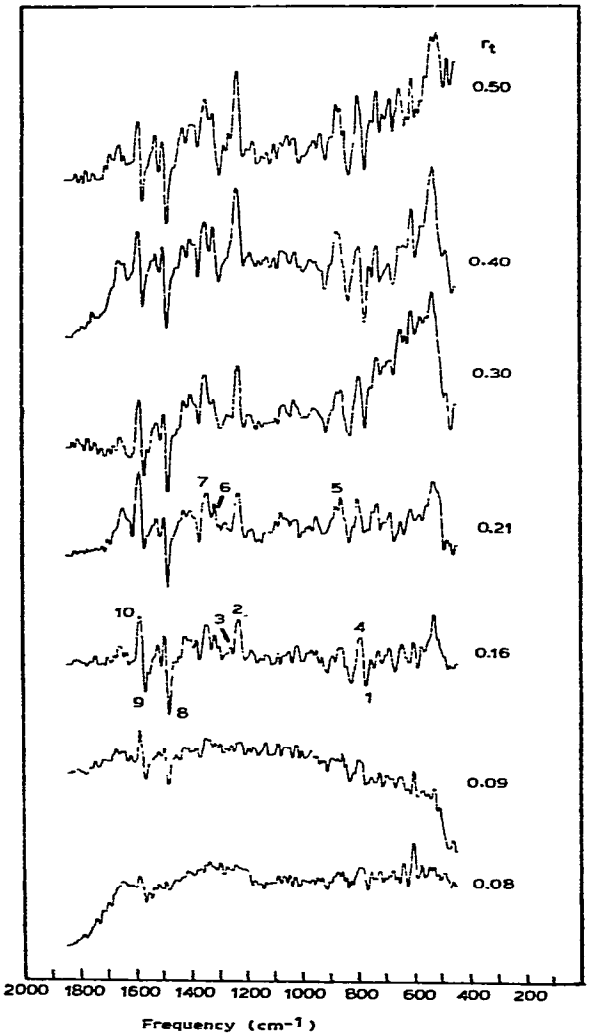

Fig. 5. Raman difference spectra of calf thymus DNA reacted with *cis*-DDP. These spectra were formed by subtraction of the $r_t = 0$ spectrum from the higher r_t value spectra. The spectral slit width was 5.4 cm^{-1} at 647.1 nm. The r_t values are indicated on the figure. Data were obtained by scanning at 20 s/step in 1 cm^{-1} steps. Spectra were subjected to two-cycle, 23-point quartic, Savitsky-Golay smoothing [50]. The r_t values are indicated on the figure. The frequencies are reported in table 3. The numbered bands are: (1) 782, (2) 1239, (3) 1278, (4) 808, (5) 884, (6) 1328, (7) 1351, (8) 1489, (9) 1573 and (10) 1590 cm^{-1}.

^2H_2O, show that at r_t values below 0.2 only small changes occur for the band at 1675 cm^{-1}, which indicates binding of $CH_3Hg(II)$ to some thymine residues. However, above $r_t = 0.3$ an abrupt intensity increase in the 1675 cm^{-1} band is observed. This suggests that $CH_3Hg(II)$ may bind cooperatively to thymine residues between $r_t = 0.3$ and 0.5.

Table 3

Raman frequencies for the Raman difference spectra in figs. 5 and 6 of *cis*- and *trans*-DDP reacting with calf thymus DNA

Peaks (cm^{-1})		Valleys (cm^{-1})	
cis-DDP (r_t = 0.50)	*trans*-DDP (r_t = 0.35)	*cis*-DDP (r_t = 0.50)	*trans*-DDP r_t = 0.35)
491 m	–	782 s	779 s
529 vs	–	833 s	835 s
–	540 s	1489 vs	1486 vs
–	592 w	1573 s	1571 s
–	653 w		
694 w	690 w		
740 m	736 m		
808 m	801 m		
884 m	878 m		
941 m	944 m		
–	1029 m		
1058	–		
–	1081 w		
1102 w	–		
1132 w	1128 w		
–	1158 w		
1181 m	–		
–	1194 m		
1239 vs	1236 vs		
1278 w	1281 w		
1328 s	1327 m		
1351 vs	1351 vs		
1399 s	1391 s		
1432 m	1431 m		
1505 m	1500 m-s		
1531 m	1524 m		
1590 s	1588 s		
1658 m	1664 m		

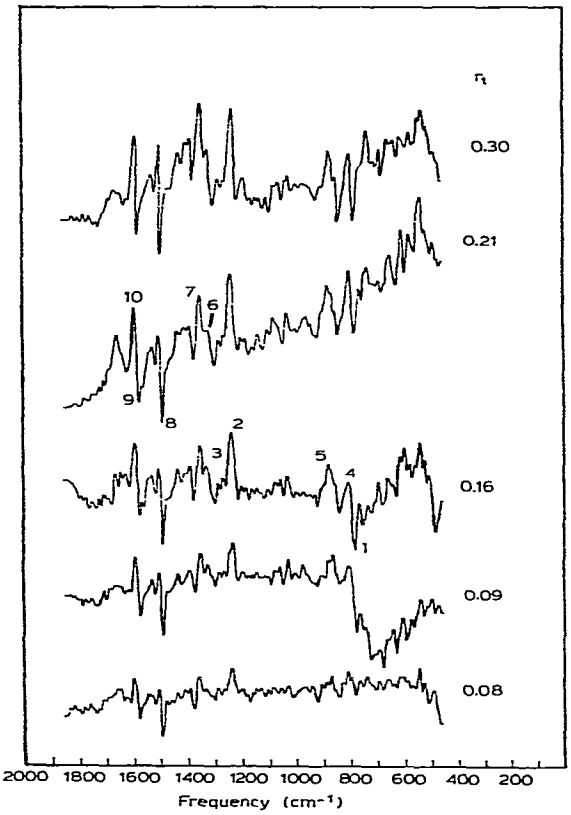

Fig. 6. Raman difference spectra of calf thymus DNA reacted with *trans*-DDP. The spectra were formed by subtraction of the r_t = 0 spectrum from the higher r_t value spectra. The spectral slit width was 6.0 cm^{-1} at 647.1 nm. The r_t values are indicated on the figure. Data were obtained by scanning at 20 s/step in 1 cm^{-1} steps. Spectra were subjected to two-cycle, 23-point quartic, Savitsky-Golay smoothing [50]. The frequencies are reported in table 3. The numbered bands are: (1) 779, (2) 1236, (3) 1281, (4) 801, (5) 878, (6) 1327, (7) 1351, (8) 1486, (9) 1571 and 1588 cm^{-1}.

At r_t values above 0.5, binding to the N(3) of cytosine is noted by following the intensity change in the band at 1247 cm^{-1} (fig. 3).

Our observations suggest that the order of $CH_3Hg(II)$ binding to bases in double-stranded DNA is G ≥ T > C > A.

The thermodynamics and kinetics for $CH_3Hg(II)$ reacting with nucleic acid constituents predict initial binding to thymine residues based on the similarity of thymine and uracil residues [13,40]. In fact, with a DNA model system and heat-denatured DNA, the initial binding site of $CH_3Hg(II)$ is the N(3) of thymine [10,11]. Since our results indicate that the initial binding site of $CH_3Hg(II)$ is the N(1) of guanine residues, when native DNA is the nucleophile, it appears that the secondary structure of DNA may play a role in directing the binding of $CH_3Hg(II)$, selectively, to the N(1) of guanine.

We have also investigated the effect of $CH_3Hg(II)$ binding on the secondary structure of

DNA. Several bands for each of the bases exhibit increases in intensity when the stacking bases decrease [41–43]. Those bands monitor Raman hypochromism and are observed on denaturation or melting of all ordered multiple- and single-stranded polynucleotides [41–44]. The Raman difference spectra in fig. 3 show an increase in intensity of the band at 728 cm^{-1} of adenine which is associated with a decrease in adenine base stacking [41–44] observed at r_t values above 0.1; none of the other base bands exhibit distinct hypochromism without any effect from metalation. The decrease in adenine base stacking suggests that the DNA secondary structure changes above $r_t = 0.1$.

In addition to the band at 728 cm^{-1} affected by base stacking, we analyzed the 835 cm^{-1} band which is sensitive to the DNA backbone conformation. The conformation band intensity decreases between $r_t = 0.2$ and 0.3. This is consistent with an alteration of B-form DNA upon metalation.

3.3. Binding of cis-DDP and trans-DDP to calf thymus DNA

We then used the Raman difference spectrum fingerprints (fig. 2) to compare the binding of *cis*- and *trans*-DDP to calf thymus DNA. This was done in two different ways. First we examined the Raman difference spectrum for each isomer at low r_t values. Second, we constructed plots which followed intensity changes as a function of r_t for bands sensitive to base binding, base stacking, or backbone structure.

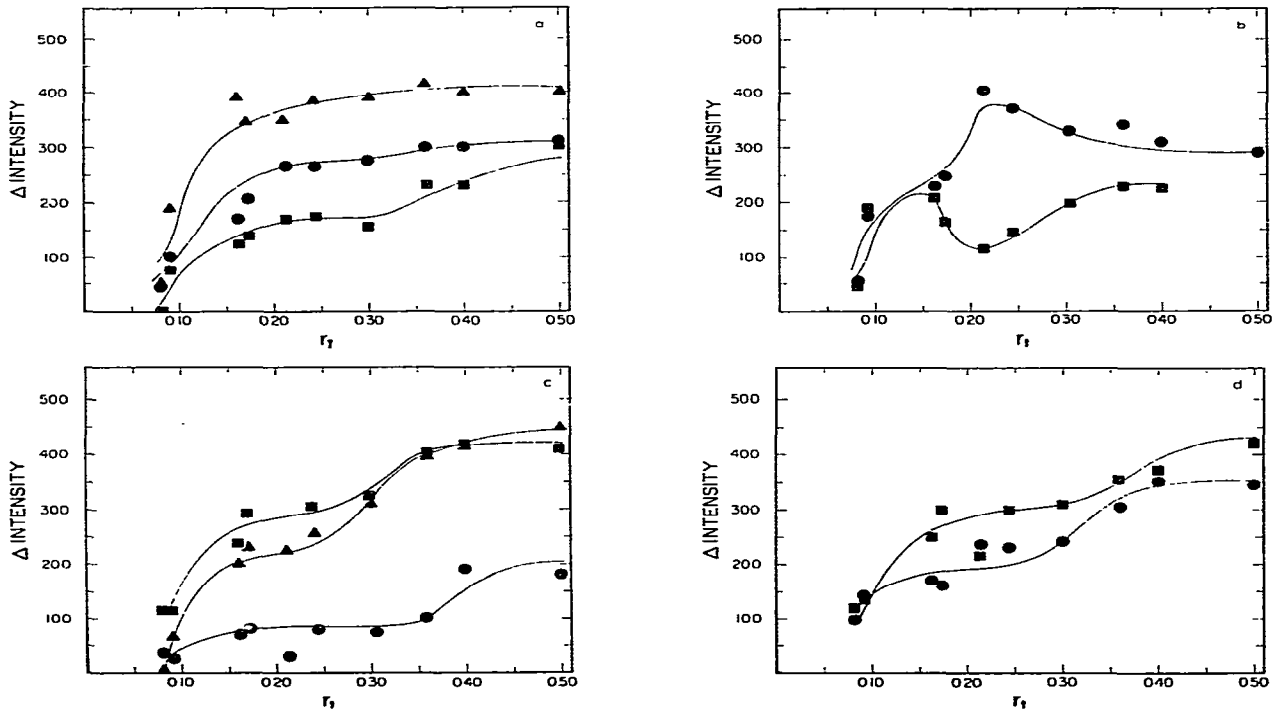

Fig. 7. Absolute intensity versus r_t plots for calf thymus DNA reacted with *cis*-DDP. The intensity values were obtained from the difference spectra in fig. 5. Difference spectra were constructed by using the $r_t = 0$ spectrum as a constant and expressing as a ratio the $r_t > 0$ spectra. The sign of the difference intensity is indicated below. The ordinate scale is in arbitrary units. (a) 1328 (■, +), 1351 (●, +), 1489 (▲, −) cm^{-1}; (b) 1573 (■, −), 1590 (●, +) cm^{-1}; (c) 782 (■, −), 1239 (▲, +), 1278 (●, +) cm^{-1}; (d) 808 (■, +), 884 (●, +) cm^{-1}.

At $r_t = 0.08$, the Raman difference spectrum of the *cis*-DDP exhibits three bands at 1489, 1573 and 1590 cm^{-1} (fig. 5). This corresponds to binding of the *cis* isomer only to guanine residues; the intense positive band at 1590 cm^{-1} in fig. 5 indicates that the *cis*-DDP reacts at the N(7) of guanine bases in double-stranded DNA (fig. 2). When the *trans*-DDP is reacted with calf thymus DNA at the r_t values, the Raman difference spectra in fig. 6 not only show bands at 1486, 1571 and 1588 cm^{-1} which suggest binding to guanine residues, but also at 1236, 1351 and 1530 cm^{-1}. The band at 1236 cm^{-1} indicates binding of the *trans* isomer to cytosine bases, whereas the bands at 1351 and 1530 cm^{-1} correspond to metalation of adenine. The bands at 1588, 1530 and 1236 cm^{-1} are consistent with binding of *trans*-DDP to the N(7) of guanine, the N(7) of adenine, and the N(3) of cytosine, respectively (fig. 2). The differences in the binding of the two isomers to DNA are even more pronounced at a slightly higher r_t value (r_t = 0.09) (figs. 5 and 6).

As the concentration of *cis*-DDP is increased above $r_t = 0.16$, however, there is evidence for reaction not only at guanine bases, but also at adenine and cytosine bases (fig. 5). We have compared the binding of *cis*- and *trans*-DDP to calf thymus DNA in a second way by plotting the changes in the absolute difference intensities against the r_t values in figs. 7 and 8. The intensity changes of the bands at 1489, 1573 and 1590 cm^{-1} (fig. 7b), those at higher r_t values seem to result more from alterations in base stacking interactions than further reaction of *cis*-DDP at guanine bases

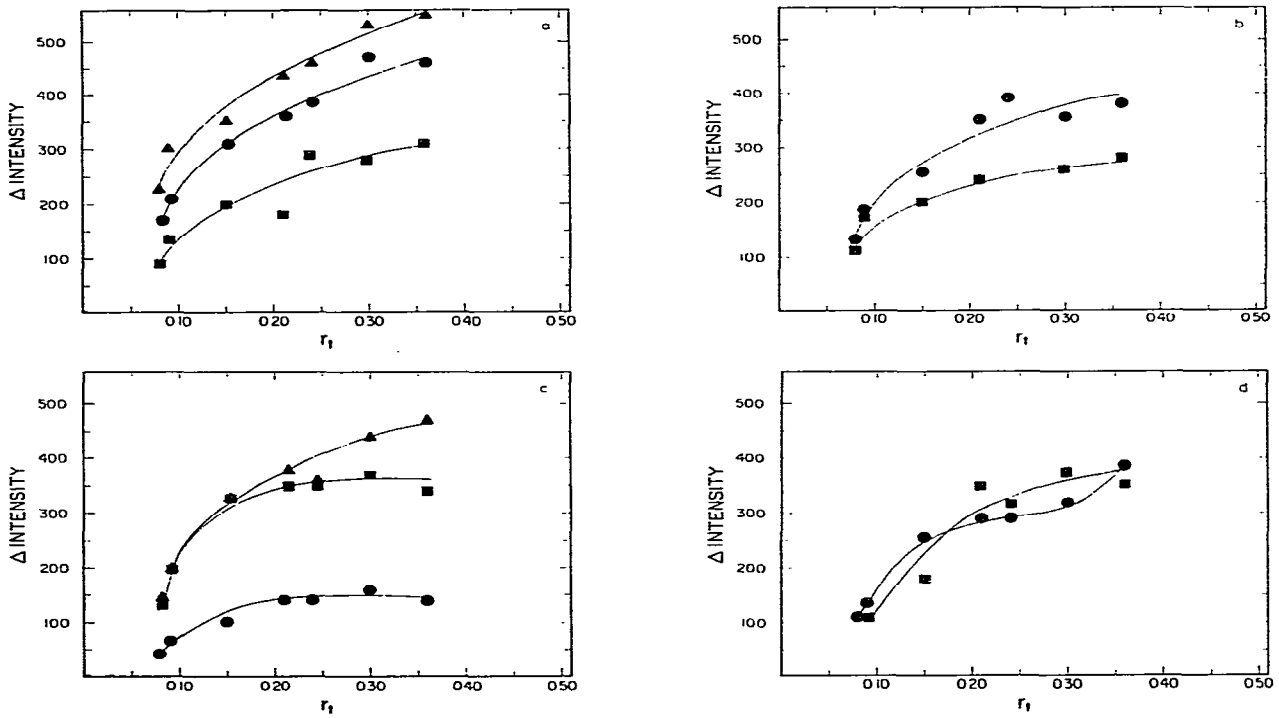

Fig. 8. Absolute intensity versus r_t plots for calf thymus DNA reacted with *trans*-DDP. The intensity values were obtained from the difference spectra in fig. 6. Difference spectra were constructed by using the $r_t = 0$ spectrum as a constant and expressing as a ratio the $r_t > 0$ spectra. The sign of the difference intensity is indicated below. The ordinate scale is in arbitrary units. (1) 1327 (■, +), 1351 (▲, +), 1486 (●, −) cm^{-1}; (b) 1571 (■, −), 1588 (●, +) cm^{-1}; (c) 779 (■, −), 1236 (●, +), 1281 (▲, +) cm^{-1}; (d) 801 (■, +), 878 (●, +) cm^{-1}.

of DNA. In contrast to the binding of *cis*-DDP, *trans*-DDP appears to bind at guanine residues over a wide r_t range as evidenced by the gradual intensity increase following the sharp initial increase for the bands at 1486, 1571 and 1588 cm^{-1} (Fig. 8a and b).

In addition to the guanine bands, the absolute difference intensities of other bands were plotted as a function of r_t. The plots of the bands at 1328, 782, 1239 and 1278 cm^{-1} in fig. 7a and 7c for the *cis*-DDP-reacted DNA present information on binding to adenine and cytosine residues. Between $r_t = 0.16$ and 0.30 the intensity of the above-mentioned bands is relatively constant. The intensities increase radically, however, above $r_t = 0.30$. Those biphasic transitions may occur as a result of increased metalation at adenine (1328 cm^{-1}) and cytosine (782, 1239 and 1278 cm^{-1}). The bands at 782, 1239 and 1328 cm^{-1} may also have contributions from hypochromism caused by a reduction in base stacking.

The plots of absolute difference intensity versus r_t value for the reaction of *trans*-DDP with DNA (fig. 8a and c), however, do not show the biphasic transitions observed for the *cis*-DDP reaction. The gradual intensity increases upon *trans*-DDP binding observed for adenine (1327 cm^{-1}) and cytosine (779, 1236 and 1281 cm^{-1}) are consistent with nonselective binding of *trans*-DDP to guanine, cytosine and adenine bases over the r_t range studied.

Although conditional formation constants from Raman studies have shown Pt(II) binding to thymine residues at N(3) to be favored over the other three bases [45,47], Pt(II) is an inert electrophile, and the deprotonation associated with Pt(II) binding to the N(3) of thymine makes that reaction extremely slow [26]. Consequently, no perturbations associated with thymine binding to *cis*- or *trans*-DDP are found in the spectra in this investigation. That is consistent with the observation that the reactions of *cis*-DDP and *trans*-DDP are controlled to a great extent by kinetics [11], i.e., the predominant reaction products are the first products to form.

Our observations suggest that the order of binding of *cis*-DDP to native calf thymus DNA is $G > A \approx C \gg T$. The order of *trans*-DDP binding

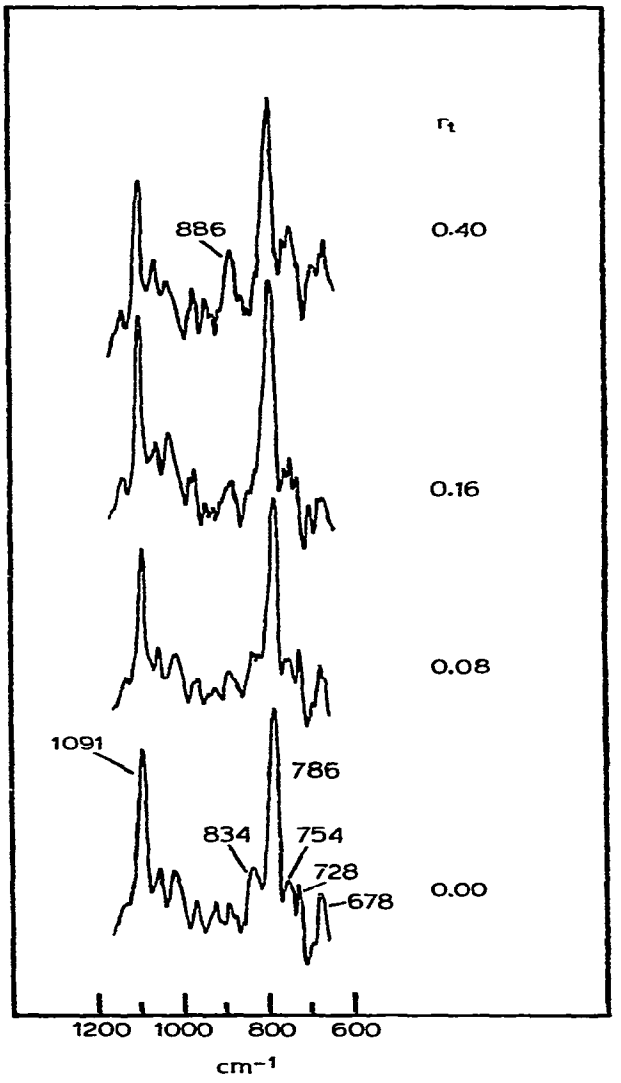

Fig. 9. Raman spectra of calf thymus DNA (12.1 mM phosphate) reacted with *cis*-DDP, pH 7.4, $[Na(CH_3)_2AsO_2] = 4$ mM. The spectral slitwidth was 5.4 cm^{-1} at 647.1 nm. The r_t values are indicated on the figure. Data were obtained by scanning at 20 s/step in 1 cm^{-1} steps. Spectra were subjected to one-cycle, 23-point quartic, Savitsky-Golay smoothing [50]. The frequencies are indicated in table 4. These spectra were formed by the subtraction of solvent water background. The frequency values in wave numbers (cm^{-1}) are indicated on the figure.

to native calf thymus DNA, however, is different: $G \approx A \approx C \gg T$.

Besides the determination of binding sites, the Raman difference spectra in figs. 5 and 6 also show that binding of *cis*- or *trans*-DDP can dramatically alter the backbone conformation of calf thymus DNA from the B form. The backbone conformational bands are generally located between 800 and 900 cm^{-1} [46]. The appearance of 884 and 878 cm^{-1} bands in the Raman difference spectra in figs. 5 and 6, respectively, is consistent with the formation of C-type DNA [46]. To demonstrate that the loss of B-DNA is concomitant with the appearance of C-DNA, we have included the Raman spectra of calf thymus as a function of r_t for *cis*-DDP (fig. 9) and plotted difference intensity versus r_t for conformationally related bands at 808 and 884 cm^{-1} (fig. 7d). The band at 834 cm^{-1} depicts B-DNA, whereas the band at 886 cm^{-1} described C-DNA [46]. The Raman spectra of *trans*-DDP reacted with calf thymus DNA appear very similar to those produced by the *cis*-DDP reaction (not shown). The plots of absolute difference intensity in fig. 7d show that *cis*-DDP binding causes a biphasic transition in both bands associated with conformation, in contrast to the effect of the *trans*-DDP which seems to cause only one conformational transition (fig. 8d). The second transition of *trans*-DDP may not be realized, however, because at $r_t \geq 0.4$ the *trans*-DPP-DNA complex precipitates. Overall, the more compact C structure [48] may be caused by a reduction in the charge of the chains (by the binding of a $Pt(II)^{2+}$ complex) which permits closer approach of the phosphates.

The observation of C-form DNA upon *cis*- and *trans*-DDP binding may prove significant in the future, because different forms of DNA may play a role in gene expression [49]. Thus, the effectiveness of *cis*-DDP as a drug may partially be related to its ability to induce the C conformation.

Acknowledgements

This work was supported by the National Institutes of Health and the American Cancer Society.

References

1 G.L. Eichhorn, in: Metal ions in biological system, vol. 10, ed. H. Sigel (Marcel Dekker, New York, 1980) ch. 1.
2 C.P. Fiessel, A. Furst and S.B. Radding, in: Metal ions in biological systems, vol. 10, ed. H. Sigel (Marcel Dekker, New York, 1980) ch. 2.
3 M.J. Cleare and P.C. Hydes, in: Metal ions in biological systems, vol. 11, ed. H. Sigel (Marcel Dekker, New York, 1980) ch. 1.
4 M.E. Howe-Grant and S.J. Lippard, in: Metal ions in biological systems, vol. 11, ed. H. Sigel (Marcel Dekker, New York, 1980) ch. 2.
5 L.G. Marzilli, Prog. Inorg. Chem. 23 (1977) 255.
6 S. Mansy, T.E. Wood, J.C. Sprowles and R.S. Tobias, J. Am. Chem. Soc. 96 (1974) 1762.
7 S. Mansy and R.S. Tobias, J. Am. Chem. Soc. 96 (1974) 6874.
8 S. Mansy and R.S. Tobias, Inorg. Chem. 14 (1975) 287.
9 S. Mansy, J.P. Frick and R.S. Tobias, Biochim. Biophys. Acta 378 (1975) 319.
10 R.W. Chrisman, S. Mansy, H.J. Peresie, A. Ranade, T.A. Berg and R.S. Tobias, Bioinorg. Chem. 7 (1977) 245.
11 M.R. Moller, M.A. Bruck, T. O'Connor, F.J. Armatis, Jr, E.A. Knolinski, N. Kottmair and R.S. Tobias, J. Am. Chem. Soc. 102 (1980) 4589.
12 D.W. Gruenwedel and N. Davidson, J. Mol. Biol. 21 (1966) 129.
13 R.B. Simpson, J. Am. Chem. Soc. 86 (1964) 2059.
14 B. Rosenberg, E. Renshaw, L. Van Camp, J. Hartwick and J. Drobnick, J. Bacteriol. 93 (1967) 716.
15 B. Rosenberg, L. Van Camp, E. Grimley and A.J. Thomson, J. Biol. Chem. 242 (1967) 1347.
16 B. Rosenberg and L. Van Camp, Cancer Res. 30 (1970) 1799.
17 H.C. Harder and G.R. Gale, Int. J. Cancer 6 (1970) 207.
18 J.A. Howle and G.R. Gale, Biochem. Pharmacol. 19 (1970) 2757.
19 B. Rosenberg, L. Van Camp, J.E. Trosko and V.H. Mansour, Nature 222 (1969) 385.
20 M.J. Cleare and P.C. Hydes, in: Metal ions in biological systems, vol. 11, ed. H. Sigel (Marcel Dekker, New York, 1980) ch. 1.
21 J.J. Roberts and A.J. Thomson, Prog. Nucleic Acid Res. 22 (1979) 71.
22 S.H. Kim, F.L. Suddath, G.J. Quigley, A. McPherson, J.L. Sussman, A.H.J. Wang, N.C. Seeman and A. Rich, Science 185 (1974) 435.
23 J.D. Robertus, J.E. Ladner, J.T. Finch, D. Rhodes, R.S. Brown, B.F.C. Clark and A. Klug, Nature 250 (1974) 546.
24 C.D. Stout, H. Mizuno, J. Rubin, T. Brennau, S.T. Rao and M. Sundaralingam, Nucleic Acid Res. 3 (1976) 1111.
25 R. Wing, H. Drew, T. Takano, C. Broka, S. Tanaka, K. Itakura and R.E. Dickerson, Nature 287 (1980) 755.
26 S. Mansy, G.Y.H. Chu, R.E. Duncan and R.S. Tobias, J. Am. Chem. Soc. 100 (1978) 607.

27 a T. O'Connor, S. Mansy, M. Bina, D.R. McMillin, M.A. Bruck and R.S. Tobias, Biophys. Chem. 15 (1982) 53;
b R.J. Douthart, S. Mansy, R.W. Schär, T. O'Connor and R.S. Tobias, manuscript in preparation. .
28 A.J.P. Alix, L. Bernard, M. Manfait, P.K. Ganguli and T. Theophanides, Inorg. Chim. Acta 55 (1981) 147.
29 S.C. Dhara, Indian J. Chem. 8 (1970) 143.
30 G.B. Kauffman and D.O. Cowan, Inorg. Synth. 7 (1963) 239.
31 J.D. Hoeschele, The preparation, purification, and analyses of *cis*-$[PtCl_2(NH_3)_2]$, Biophysics Department, Michigan State University, East Lansing, MI, 1911.
32 H.R. Mahler, B. Kline and B.D. Mehrota, J. Mol. Biol. 9 (1964) 801.
33 J.W. Lundeen, Ph.D. Thesis, Purdue University (1974).
34 T.H. Bushaw, Ph.D. Thesis, Purdue University (1979).
35 J.W. Amy, R.W. Chrisman, J.W. Lundeen, T.Y. Ridley, J.C. Sprowles and R.S. Tobias, Appl. Spectrosc. 28 (1974) 262.
36 R.W. Chrisman, J.C. English and R.S. Tobias, Appl. Spectrosc. 30 (1976) 168.
37 F. Basolo and R.G. Pearson, Mechanisms of inorganic reactions, 2nd edn. (Wiley, New York, 1967).
38 R.M. Izatt, J.J. Christensen and J.H. Rytting, Chem. Rev. 71 (1971) 439.
39 M.R. Moller, Ph.D. Thesis, Purdue University (1979).
40 a G. Geier and I.W. Erni, Chimia 27 (1973) 635;
b G. Geier, I. Erni and R. Steiner, Helv. Chim. Acta 60 (1977) 9;
c A. Evans, D.L. Rabenstein, G. Geier and I. Erni, J. Am. Chem. Soc. 99 (1977) 8106.
41 P.C. Painter and J.L. Koenig, Biopolymers 15 (1976) 241.
42 L. Rimai, V.M. Maher, D. Gill, I. Salmeen and J.J. McCormick, Biochim. Biophys. Acta 361 (1974) 155.
43 S.C. Erfurth and W.L. Peticolas, Biopolymers 14 (1975) 247.
44 G.J. Thomas, Jr, in: Structure and conformation of nucleic acids and protein-nucleic acid interactions, eds. M. Sundaralingam and S.T. Rao (University Park Press, Baltimore, 1975) p. 253.
45 G.Y.H. Chu, R.E. Duncan and R.S. Tobias, Inorg. Chem. 16 (1977) 2625.
46 a S.C. Erfurth, P.J. Bond and W.L. Peticolas, Biopolymers 14 (1975) 1245;
b S.C. Erfurth, E.J. Kiser and W.L. Peticolas, Proc. Natl. Acad. Sci. U.S.A. 69 (1972) 983;
c D.C. Goodwin and J. Brahms, Nucleic Acid Res. 5 (1978) 835.
47 W.M. Scovell and T. O'Connor, J. Am. Chem. Soc. 99 (1977) 120.
48 D.A. Marvin, M. Spencer, M.H.F. Wilkins and L.D. Hamilton, J. Mol. Biol. 3 (1961) 547.
49 R.D. Weels, T.C. Goodman, W. Hillen, G.T. Horn, R.D. Klein, J.E. Larson, U.R. Müller, S.K. Nevendorf, N. Panayotatos and S.M. Stirdivant, Prog. Nucleic Acid Res. 24 (1980) 167.
50 a A. Savitsky and M.J.E. Golay, Anal. Chem. 36 (1964) 1627;
b H.H. Madden, Anal. Chem. 50 (1978) 1383;
c J. Steiner, Y. Termona and J. Deltour, Anal. Chem. 44 (1972) 1906.